Aberration correction: some advantages and alternatives

R.E. Dunin-Borkowski,[1] T. Kasama,[2] L. Cervera,[1] A.C. Twitchett,[1] P.A. Midgley,[1] A.C. Robins,[3] D.W. Smith,[3] J.J. Gronsky,[3] C.M. Thomas,[3] P.E. Fischione,[3] C.J.D. Hetherington,[4] A.I. Kirkland[4]

[1] Department of Materials Science and Metallurgy, Pembroke Street, Cambridge CB2 3QZ, UK
[2] RIKEN, 2-1 Hirosawa, Wako, Saitama 351-0198, Japan
[3] E.A. Fischione Instruments, Inc. 9003 Corporate Circle, Export, PA 15632
[4] Department of Materials, Parks Road, Oxford OX1 3PH, UK

The resources that have been invested in the development of aberration-corrected transmission electron microscopes (TEMs) are bearing fruit, with the advantages of using objective correctors for imaging nanoscale materials including a decrease in image delocalization, as illustrated in Fig. 1 for lattice images of a Pt nanoparticle recorded at 200 kV using spherical aberration coefficients of -20 and 450 μm. A notable feature of the corrected images is an increase in background intensity in the particle, suggesting that without correction many of the electrons that have been scattered to high angles may be excluded from the final image, and that the ubiquitous discrepancy between the contrast of experimental lattice images and simulations (the "Stobbs factor") may be reduced when aberration correction is used.

Equally important are advances in the design of specimen holders, instrument control, image processing and image analysis that can be implemented in conjunction with (or instead of) aberration correction. Figure 2 shows design drawings for two ultra-high-tilt electrical biasing specimen holders, which we are using to apply electron holography with electron tomography to characterize electrostatic and magnetic fields in working devices in three dimensions, as currents flow through them *in situ* in the electron microscope. Samples are held in removable cartridges that are interchangeable between transmission and scanning microscopes, as well as between focused ion beam workstations, ion millers and plasma cleaners. The holder shown in Fig. 2a allows a semiconductor device to be examined under an applied bias using electron tomography and electron holography. The removable cartridge (Fig. 2b) is used to make electrical contacts to the front and back surfaces of a cleaved square of semiconductor wafer, whose thin edge has been thinned using focused ion beam (FIB) milling, via a small conducting block and a second spring contact. In the TEM, tilts of $\pm 80^\circ$ can be achieved before the region of interest on the sample is obscured by the edges of the holder. Figure 3a show defocused images of an FIB-prepared Si p-n junction, acquired for a range of reverse and forward bias voltages applied across the junction. The holder shown in Fig. 2b allows the same techniques to be applied to a specimen with contact pads on its surfaces, towards which a third contact can be moved using micrometers or piezoelectric drives. Figure 3b shows a defocused image of a biased carbon nanotube, of interest for field emission applications, acquired using this holder. Either holder can be used for three-dimensional induction mapping inside magnetic nanostructures. Two ultra-high-tilt series of electron holograms about orthogonal axes are then required to provide the three-dimensional distribution of two of the three components of the induction within and around a sample. The third component can be evaluated by making use of the criterion that $\nabla.\mathbf{B} = 0$. The ability to acquire holograms of magnetic particles about orthogonal axes is illustrated in Fig. 3c.

We thank the Royal Society, the EPSRC and Newnham College, Cambridge for financial support, Stephan Hofmann, Jonathan Barnard, Stuart Holmes and Ronald Broom for assistance, and Johnson Matthey (Sonning Common) and Philips Research (Eindhoven) for samples.

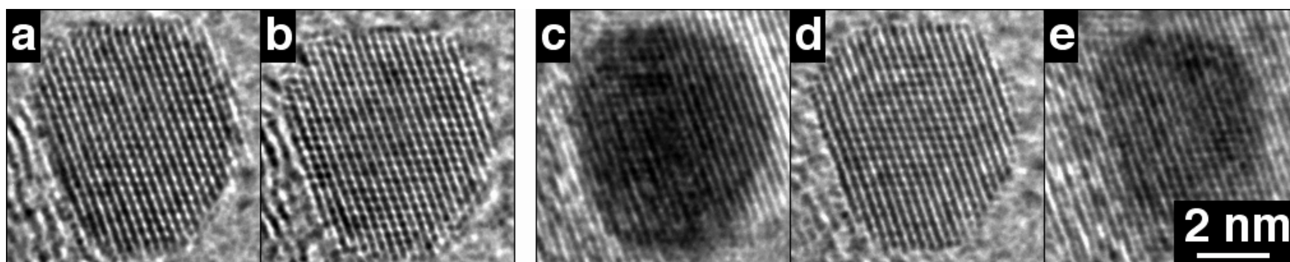

FIG. 1. Lattice images of a 5 nm Pt particle recorded at 200 kV using a JEOL 2200FS field emission gun TEM. Images a) and b) were recorded at defocus values of -93 and -148 nm with C_S set to -20 µm. Images c), d) and e) were recorded at defocus values of -87, -117 and -194 nm with C_S set to 450 µm. The defoci are measured from the carbon film, which is at a different height to the particle.

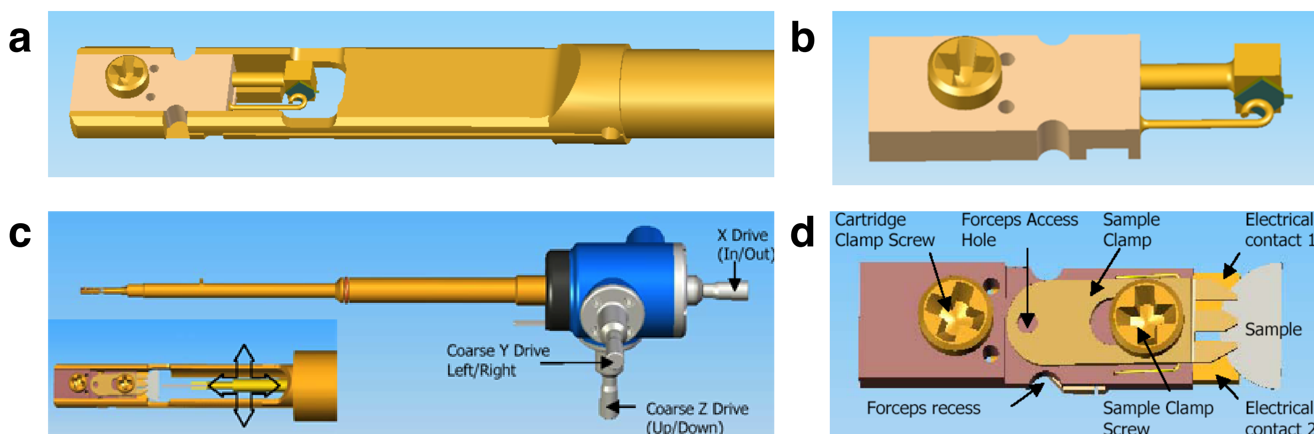

FIG. 2. a) Design drawing of the end of an ultra-high-tilt two-contact cartridge-based electrical biasing holder. b) The cartridge with a cleaved FIB-milled sample in place. c) Design drawing of an ultra-high-tilt three-contact cartridge-based electrical biasing nanopositioning holder, with three-axis movement of the probe provided by micrometers and piezoelectric crystals. d) The cartridge with a sample resting on two electrical contacts. All three contacts are isolated from the body of the holder.

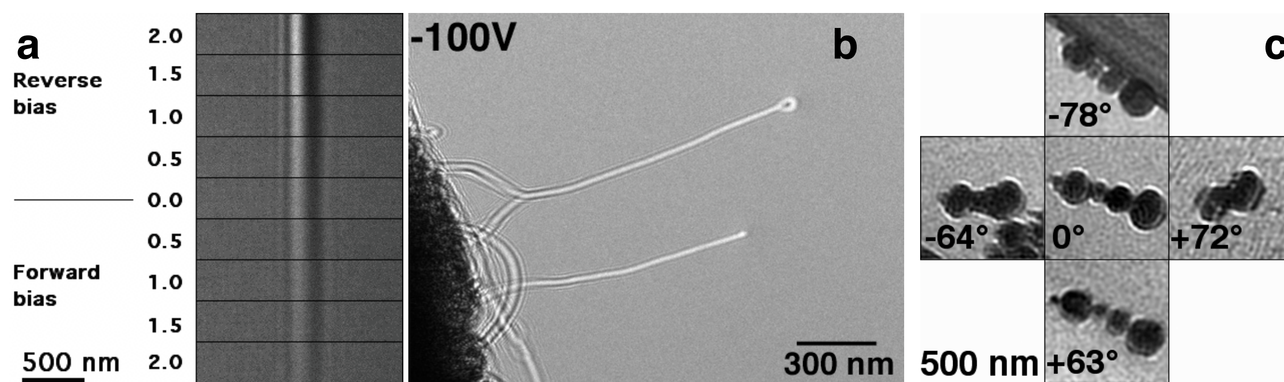

FIG. 3. a) Montage of energy-filtered images of a 10^{18}cm^{-3} abrupt Si p-n junction acquired using the holder shown in Fig. 2a vs applied voltage at -3.5 mm defocus. b) Defocused image of a carbon nanotube with 100 V between the nanotube and a gold wire mounted on the probe in the holder shown in Fig. 2c. c) Amplitude images reconstructed from electron holograms of FeNi nanocrystals, acquired in field-free conditions at the tilts indicated about orthogonal axes from the central image.